

## A simple model of the magnetic emission from a dust devil

Michael V. Kurgansky,<sup>1,2</sup> Leonardo Baez,<sup>1</sup> and Elías M. Ovalle<sup>1</sup>

Received 7 June 2007; revised 20 August 2007; accepted 9 October 2007; published 27 November 2007.

[1] A simple Rankine-like vortex model of the dust devil behaving as a magnetic solenoid has been constructed. It is augmented with a one-dimensional model describing steady vertical distribution of the electric charge in the dust devil. For terrestrial dust devils, the model permits uniform vertical distribution of the negatively charged dust within the main vortex flow. For higher electric conductivity of air on Mars, the model hints on a rapid decay with altitude of the dust electrification, with e-folding height order of several tens of meters, which is much less than the total dust column height. It is shown that some characteristic features of recently discovered ULF magnetic emission from the terrestrial dust devil can be interpreted in terms of interaction between negatively charged smaller-scale vortex filaments inside the main vortex. It is conjectured that such ULF magnetic emission should be accompanied by the emission of sound waves of approximately doubled frequency.

**Citation:** Kurgansky, M. V., L. Baez, and E. M. Ovalle (2007), A simple model of the magnetic emission from a dust devil, *J. Geophys. Res.*, 112, E11008, doi:10.1029/2007JE002952.

### 1. Introduction

[2] Recently, an ULF magnetic emission from terrestrial dust devils has been discovered [Houser *et al.*, 2003; Farrell *et al.*, 2004]. Houser *et al.* [2003] originally detected broadbanded ULF magnetic emission from a dust devil, at frequencies below 50 Hz and with peaks near 10 Hz, whereas a second dust devil detected by Farrell *et al.* [2004] produced surprisingly narrowbanded ULF emission between 1 and 10 Hz with a distinct peak at a 3 Hz. Houser *et al.* [2003] suggested that this ULF magnetic emission is the result of the cyclonic motion of the charged grains in the dust devil behaving as a magnetic solenoid. On the basis of this idea, Farrell *et al.* [2004] provided a simple, order-of-magnitude estimate of the magnetic field from a solenoid dust devil generator.

[3] In this note, we further develop this approach by considering a Rankine-like vortex, with its radius increasing with height, to mimic the dust devil vortex structure [Kurgansky, 2005], and by adjusting this specific fluid dynamical model for magnetic emission studies. We shall also augment the magnetic solenoid dust devil model with a simple, but self-consistent, account for dust devil updrafts shaping the electric charge vertical distribution in the presence of the atmospheric electric conductivity. The constructed model explains a DC (direct current) magnetic flux density near the ground, which is order of the observed magnetic field values [Houser *et al.*, 2003; Farrell *et al.*, 2004]. This model is aimed at further developing theoretical

backgrounds of remote sensing of dust devils and also at estimating possible magnetic signatures of dust devils on Mars. In the latter case, due to higher electric conductivity of the Martian atmosphere, we shall be forced to modify our arguments by considering an exponential vertical distribution of charged grains within the dust devil vortex.

[4] In our electromagnetic model, we shall use the empirical evidence (and the results of some theoretical models) that a clear charge separation occurs within the dust devil due to triboelectric processes, where the lighter negative charged particles are distributed in the upper part of the dust devil and participate in the swirling motion, while the heavier positive charged particles remain near the ground in a saltation regime. This physical stationary picture, namely the sense of charge separation in triboelectric processes, has also been confirmed by laboratory experiments [see, e.g., Farrell *et al.*, 2004, and references therein]. A discussion of the modeling of the transient tribocharging spin-up process in dust devils/dust storms has recently been reported by Zhai *et al.* [2006].

[5] The formation of electric dust devils is a complex multiphysical process involving vortex dynamics/thermodynamics and dust grain contact electrification and charge separation. In our work, we schematize this process as follows. Very hot surface-adjacent air parcels give rise to localized rotating thermals, or vertical vortices. They are characterized by strong wind convergence occurring within a thin surface adjacent sub-layer and by vertical velocity maximum at the altitude of a few meters above the ground. Owing to converging winds, initially electrically neutral small-size dust grains, which are suspended in air, pass through the vortex center with the strongest winds, collide with larger, and heavier, dust particles which are in saltation there, acquire the negative charge by triboelectric processes (whereas heavier grains obtain the equal by magnitude positive electric charge) and, finally, are transported upward

<sup>1</sup>Department of Geophysics, Faculty of Physical and Mathematical Sciences, University of Concepción, Concepción, Chile.

<sup>2</sup>On leave from A.M. Obukhov Institute of Atmospheric Physics, Russian Academy of Sciences, Moscow, Russia.

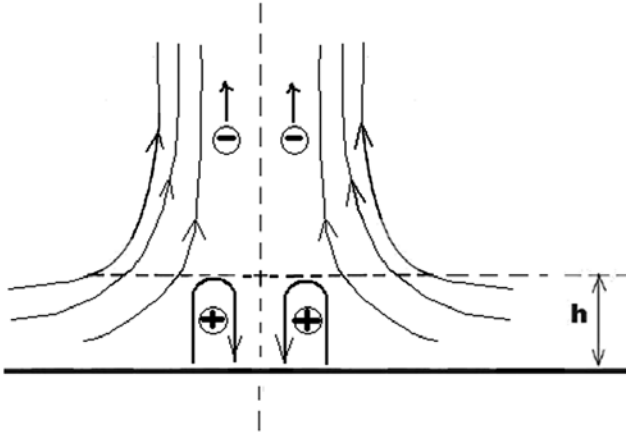


**Figure 1.** Schematic of a triboelectrostatic generator acting in a steady vortex; owing to converging winds, initially noncharged small-size dust grains pass through the saltation zone, collide there with heavier dust particles, acquire negative charge by triboelectric processes, and afterward are transported by wind upward. A steady saturated state, as well as the overall electric neutrality, is maintained by Ohmic dissipation due to electric conductivity of air, which acts (1) on a microscopic level within the active triboelectrification (saltation) region of height  $h$  and (2) on a macroscopic level within the upper vortex flow (see more in section 3).

by wind (Figure 1). A steady saturated state within the dust devil, as well as the overall electric neutrality, is maintained by Ohmic dissipation due to electric conductivity of air, which effectively acts (1) on a small scale within the triboelectrification (saltation) region and (2) on a large scale within the upper vortex flow (see more in section 3).

[6] From the perspective of electrodynamics, the principal contribution to the magnetic field generation in a steady dust devil comes from the negatively charged lighter particles, which participate in the swirling motion. Only their cyclonic motion is explicitly considered in our model, as the mechanism of magnetic field generation. Of course, by electric charge conservation, some parasitic electric currents will inevitably be produced in the bottom zone, where the effect of tribocharging is dominant. In this way, the global electric neutrality of the dust devil is secured. It is especially true when some transient events, or imbalances, occur within the electric dust devil. However, we consider that the magnetic field produced in the bottom zone is negligible compared to the magnetic field produced in the upper zone and will not be considered in our analysis.

[7] A crucial pending task is to explain an AC (alternating current) magnetic field emission, as measured in terrestrial dust devils. To do it, *Farrell et al.* [2006] developed a numerical model, in which an AC magnetic field generation is explained by essentially different behavior, in a swirling driving flow, of positively charged coarse-grained dust, on the one hand, and negatively charged fine-grained dust, on the other hand. A vertical wind was also included and the simulation was initially seeded with a number of isolated clumps of dust grains.

[8] An alternative theoretical possibility, explored hereafter, would be to consider multiple smaller-scale whirls of the same sense of vorticity within the main dust devil vortex (compare to “suction vortices” in tornadoes [*Fujita*, 1981]; see also *Bluestein* [2005]), which can also be considered as negatively electrically charged filaments. If they carry different negative electric charges and interact dynamically pair-wise, by rapidly rotating about the common center of vorticity, then these vortex/electric filament interactions can explain certain characteristic features of the observed ULF magnetic emission. These interacting filaments must also emit sound waves (the Lighthill emission [see *Crighton*, 1981]) of measurable magnitude, with the frequency twice as high as that of the magnetic emission. It could serve as an observational test for the proposed mechanism validity.

## 2. Dust Devil as a Magnetic Solenoid

[9] The Maxwell equations of electrodynamics in terms of an electric field  $\mathbf{E}$  and a magnetic field  $\mathbf{B}$  read

$$\begin{aligned} \nabla \cdot \mathbf{E} &= \rho_e / \epsilon_0, & \nabla \cdot \mathbf{B} &= 0, & \nabla \times \mathbf{B} &= \mu_0 \mathbf{j} + \mu_0 \epsilon_0 \partial_t \mathbf{E}, \\ & & \partial_t \mathbf{B} + \nabla \times \mathbf{E} &= 0. \end{aligned} \quad (1)$$

In our model we use the vacuum values for the magnetic permeability,  $\mu_0 = 4\pi \times 10^{-7} \text{ NA}^{-2}$ , and the electric permittivity,  $\epsilon_0 \cong 8.854 \times 10^{-12} \text{ Fm}^{-1}$ . The electric charge and current densities,  $\rho_e$  and  $\mathbf{j}$ , obey the electric charge conservation law  $\partial_t \rho_e + \nabla \cdot \mathbf{j} = 0$ . In our problem,  $\partial_t \mathbf{B}$  in the last equation (1) (Faraday’s law) is very small and an electric field  $\mathbf{E}$  is quasi-potential.

[10] Under the magnetostatic approximation, equation (1) yields  $\nabla \times \nabla \times \mathbf{A} = \mu_0 \mathbf{j}$ , where  $\mathbf{B} = \nabla \times \mathbf{A}$  and  $\mathbf{A}$  is the vector potential, such that  $\nabla \cdot \mathbf{A} = 0$ . In general cases,  $\mathbf{j} = \rho_e \mathbf{v} + \sigma \mathbf{E}$ , where  $\mathbf{v}$  is the fluid velocity and  $\sigma$  the electric conductivity. As a first approximation, we consider an airflow with only convective current,  $\mathbf{j} = \rho_e \mathbf{v}$ . We use cylindrical polar coordinates  $(r, \varphi, z)$ , with  $r$  as the radius,  $\varphi$  the azimuth and  $z$  the altitude, and consider a steady axisymmetric flow, balanced both hydrostatically and cyclostrophically. More specifically, we take a Rankine-like vortex flow with the vortex core radius  $r = r_m(z)$  depending of altitude. Inside the vortex core, at each horizontal level, the azimuthal velocity  $v$  is a linear function of the radius  $r$  and attains its maximal value  $v_m(z) = \Gamma / r_m(z)$  at  $r = r_m(z)$ . Here,  $\Gamma$  is the constant (uniform) value of angular momentum at the vortex core sidewalls. Outside the vortex core the flow is irrotational. This purely swirling flow, without any updrafts, can serve as a crude approximation to observed dust devils. *Balme and Greeley* [2006] indicate that the vertical velocity in dust devils is generally about a quarter of the maximum swirl velocity.

[11] For a steady axisymmetric dust devil vortex, the equation

$$\frac{1}{r} \frac{\partial}{\partial r} \left( r \frac{\partial A_\varphi}{\partial r} \right) + \frac{\partial^2 A_\varphi}{\partial z^2} - \frac{1}{r^2} A_\varphi = - \frac{\mu_0 \rho_e(r, z) \Gamma r}{r_m^2(z)} \quad (2)$$

specifies the azimuthal component of vector potential  $A_\varphi = A_\varphi(r, z)$ , given  $r_m(z)$  and  $\rho_e(r, z)$ . The poloidal magnetic field then reads:  $\mathbf{B} = (-\partial A_\varphi / \partial z, 0, \partial(r A_\varphi) / r \partial r)$ .

[12] This setup uses clear electric charge separation within the dust devil. By the virtue of the tribocharging effect [see *Farrell et al.*, 2003, and references therein], the fine-grained dust becomes negatively charged, being involved into vigorous vortex motion. Positively charged coarser-grained dust is observed in the regime of saltation and remains near the ground, being not actively involved into the vortex flow. Therefore it can reasonably be assumed that electric currents in the dust devil are created exclusively by negatively charged fine-grained dust. Certainly, the heavier positive charged grains provide the overall electric neutrality within the dust devil, but they are excluded from our analysis of magnetic field emissions because they do not produce noticeable electric currents. We shall also discuss the role of positive charged grains in section 3.

[13] Besides, there is experimental evidence of dust concentration near the vortex core outer edge. The presence of dust particles in the inner part of vortex core is suppressed, most likely, by both the downdraft motion and the centrifugal force action [*Sinclair*, 1966, 1973; see also *Rennó et al.*, 1998]. Also, *Brooks* [1951] remarks how the size of the particles in a whirling column of dust or sand increases with the distance from the dust devil center. It could also be related to a system of updrafts within the core, which are not evenly distributed but concentrated in the vicinity of the vortex core sidewalls. A tendency toward such a maximum updraft location is seen in numerical simulations of Martian dust devil vortices [*Toigo et al.*, 2003]. In addition, the electrical capacitance of dust particles increases linearly with their radii, so larger airborne particles can carry more negative electric charge. In synthesis, we anticipate delta-singularity of negative electric charge distribution  $\rho_e(r, z) = [q_-(z)/2\pi r_m(z)]\delta[r - r_m(z)]$  in the right-hand side of (2). In this study, the one-dimensional negative electric charge density in the vertical direction (having units of coulomb per meter) is taken constant,  $q_-(z) = q_- = \text{const}$ . Now the solution of (2), which is regular at  $r \rightarrow \infty$  reads:  $A_\phi = Ar/r_m^2(z)$ ,  $r \leq r_m(z)$  and  $A_\phi = A/r$ ,  $r > r_m(z)$ , with  $A = (1/4\pi)\mu_0 q_- \Gamma$ . It exists only if  $\partial^2 A_\phi / \partial z^2 \equiv 0$ , i.e., either (1)  $r_m(z) = r_m = \text{const}$  or (2)  $r_m^{-2}(z) = a(H - z)$ ,  $a = \text{const}$ ,  $H = \text{const}$ . The second option corresponds to a Rankine-like vortex with its radius unlimitedly growing with altitude and becoming infinite at a limit height  $z = H$  [cf. *Kurgansky*, 2005]. The poloidal magnetic field within the vortex core,  $B_r = \mu_0 q_- \Gamma r a / 4\pi$ ,  $B_z = \mu_0 q_- \Gamma a (H - z) / 2\pi$ , corresponds to the constant vertical magnetic flux  $\Phi = 2\pi \int_0^m B_z(r) r dr = (1/2)\mu_0 q_- \Gamma$ . Outside the vortex core the magnetic field is zero.

[14] In applications to the terrestrial dust devil we assume that the zone between the ground  $z = 0$  and the altitudinal level  $z = h \ll H$  is filled in by positively charged dust observed in the saltation regime and not participating in the swirling motion. Therefore we will consider our idealized vortex solution at heights  $z \geq h$  by noting that  $r_m \equiv r_m(h) \sim h$  and using  $r_m^{-2} = aH$ . Now, the maximal magnetic flux density reads  $B_z = (1/2\pi)\mu_0 q_- \Gamma r_m^{-2}$ . For a rough estimate, we take the macroscopic electric dipole moment  $M = QD \sim 1 \text{ C m}$  of a dust devil, where  $Q$  is the absolute value of electric charge of each pole and  $D$  the vertical distance between them [cf. *Farrell et al.*, 2003]. We use  $H \approx 2D \sim 100 \text{ m}$  from the paper cited. Therefore  $|q_-| \approx Q/H \approx 2M/H^2 \sim 2 \times 10^{-4} \text{ C m}^{-1}$  and for  $\Gamma = 50 \text{ m}^2 \text{ s}^{-1}$ ,  $r_m = 5 \text{ m}$  one obtains

$B_z \sim 8.0 \times 10^{-2} \text{ nT}$ , which is order of magnitude of the measured magnetic field during the passage of a dust devil [*Houser et al.*, 2003; *Farrell et al.*, 2004].

### 3. Electric Charge Vertical Distributions

[15] The considered solenoid dust devil generator corresponds to a nonhelical vortex flow with an infinitely large swirling ratio  $S$ , commonly defined by dividing the maximal swirl velocity by the mean updraft velocity within the vortex. Atmospheric dust devils have convective updrafts, and it is of interest to extend the above-constructed model onto the case of finite swirling ratios  $S$ . We shall use an approximate solution to the problem, valid for large  $S$  but not taken too close to the critical level  $z = H$ . Namely, “one-way coupling” within the fluid dynamical problem is accounted for, when the primary swirling circulation in the vortex shapes the secondary meridional circulation, but the backward influence of the meridional circulation on the primary circulation is neglected. Accounting for “two-way coupling” provides serious difficulties, which can be overcome only in exceptional cases [cf. *Kurgansky*, 2005]. For maximal simplicity, we take the updraft flow  $w = \bar{w}(z) \equiv F/\pi r_m^2(z)$ ,  $r \leq r_m(z)$ , and  $w \equiv 0$ ,  $r > r_m(z)$ , where  $F$  is the constant vertical volumetric flux. It is possible to use more realistic updraft patterns, but it would lead only to corrections in numerical coefficients in the resulting formulas, without changing qualitatively the main result.

[16] As in section 2 we anticipate a simple vertical structure of the electric dust devil, namely the negative charge  $q_-(z)$  in region  $h < z \leq H$  and the positive charge  $q_+(z)$  in region  $0 \leq z < h$ , such that  $\int_0^h q_+(z) dz + \int_h^H q_-(z) dz = 0$ . This electric charge distribution resembles a classical plane electric capacitor, where the electric field is confined between the two plates of the capacitor but strictly vanishes outside the capacitor. Accordingly, we require  $E_z = 0$  at  $z = 0, H$  (see Figure 2). As in section 2 we take  $q_-(z) = q_- = \text{const}$  at  $h < z \leq H$ ; the positive charge distribution  $q_+(z)$  at  $0 \leq z < h$  must satisfy the neutrality condition  $\int_0^h q_+(z) dz + q_-(H - h) = 0$ . In the simplest case  $q_+(z) = q_+ = \text{const}$  this neutrality condition reads  $q_+ h + q_-(H - h) = 0$ . We further integrate the first equation (1) (Coulomb’s law) to obtain

$$\Omega = \begin{cases} \varepsilon_0^{-1} q_+ z, & 0 \leq z < h \\ -\varepsilon_0^{-1} q_-(H - z), & h < z \leq H, \end{cases} \quad (3)$$

where  $\Omega = 2\pi \int_0^\infty E_z r dr$ . The neutrality condition  $q_+ h + q_-(H - h) = 0$  provides  $\Omega$ -continuity at  $z = h$ . In the following we consider  $\Omega$ -function (3) only in vortex flow region  $h \leq z \leq H$ . Here, the vertical component of electric current density includes both the convective and the conductive terms,  $j_z = \rho_e w + \sigma E_z$ , where  $\sigma$  is the electric conductivity of air. Integration over an arbitrary horizontal cross section of the vortex gives  $J = (1/\pi) q_- F a (H - z) + \sigma \Omega$ , and therefore

$$J(z) = \frac{q_- F}{\pi} a (H - z) - \frac{\sigma q_-}{\varepsilon_0} (H - z). \quad (4)$$

The vertical electric current  $J$  vanishes when  $F = \pi(\sigma/\varepsilon_0 a)$ . We introduce an average vertical velocity  $W = F/\pi r_m^2$  at the top of saltation layer  $z = h \ll H$  (see section 2) and rewrite the

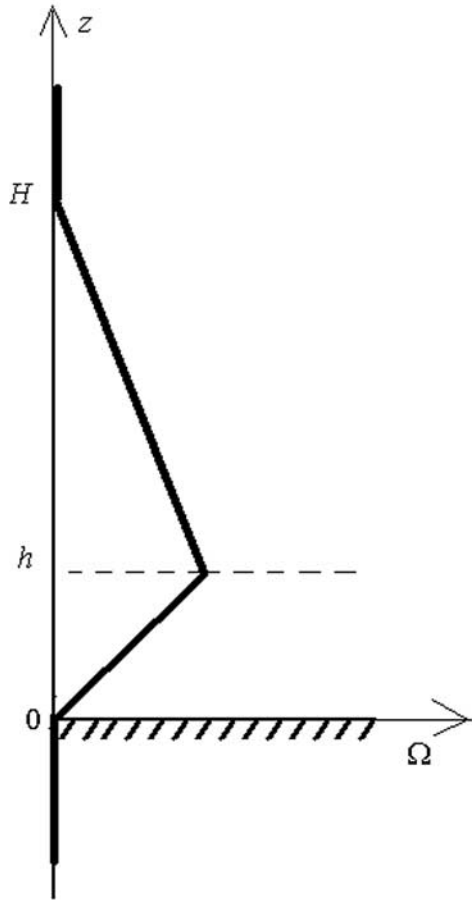


**Figure 2.** Vertical distribution of the integrated electric field  $\Omega$  (a thick solid line) (1) within the electric dust devil of finite vertical extension  $H$ , (2) above the dust devil in the neutral atmosphere,  $z > H$ , and (3) below the dust devil, i.e., under the ground,  $z < 0$ ; see formula (3) and notations in the text.

condition for  $J(z) \equiv 0$  as  $W \equiv H\sigma/\varepsilon_0$ . Making use of  $H \sim 2 \times 10^2$  m and taking the atmospheric ground-level conductivity  $\sigma \sim 6.6 \times 10^{-14}$  S m $^{-1}$  [Farrell et al., 2003] yields  $W \sim 1.5$  m s $^{-1}$ , which is comparable by magnitude with typical updraft velocities in terrestrial dust devils.

[17] Within the saltation region  $0 \leq z < h$  only heavier positively charged grains remain (whereas the lighter negatively charged grains are gone with wind upward) and we neglect both the convective and macroscopic conductive currents in this region, by assuming in the latter case that the electric conductivity of air has already been effectively accounted for on the microscopic level when considering triboelectrification of individual grains. Therefore  $J(z) \equiv 0$  and the electric charge conservation law is always satisfied.

[18] It is an exceptional case when the two flux terms in (4) cancel. In general cases, they are misbalanced, and the electric charge conservation law  $\partial_t q + \partial J/\partial z = 0$  in the vortex flow region  $h \leq z \leq H$  yields

$$\dot{q}_- = q_- \left( \frac{Fa}{\pi} - \frac{\sigma}{\varepsilon_0} \right) \equiv q_- \left( \frac{W}{H} - \frac{\sigma}{\varepsilon_0} \right), \quad (5)$$

where  $q_- = q_-(t)$  and a dot denotes the ordinary time-derivative  $d/dt$ . Equation (5) shows that the negative electric charge density  $q_-$  increases in time if  $W > H\sigma/\varepsilon_0$ . On the contrary,  $q_-$  decreases in time if  $W < H\sigma/\varepsilon_0$ . In order to maintain the overall electric neutrality of the dust devil, these temporal  $q_-$ -changes are compensated by the corresponding positive electric charge changes within saltation region  $0 \leq z < h$ , owing to the induced nonzero electric currents there (which we do not consider here in detail).

#### 4. Model Modifications for Martian Dust Devils

[19] High electric conductivity of the Martian atmosphere,  $\sigma \sim 2.5 \times 10^{-12}$  S m $^{-1}$  [Farrell and Desch, 2001], prevents applying the model of sections 2 and 3 to Martian dust devils, because it would need unrealistically high updraft velocities  $W$  to support electric charge distribution against the Ohmic dissipation. To circumvent this difficulty, a modification of the model is proposed when the negative electric charge density exponentially decays with height,  $q_-(z) = q_0 \exp[-k(z-h)]$ ,  $z \geq h$ . In this setup, we disregard the vortex core expansion with height, when  $kH \ll 1$ , and safely take  $r_m(z) = r_m = \text{const}$  (see Figure 3). Again, assuming delta-singularity of electric charge distribution at  $r = r_m$ , we obtain the solution of (2)

$$A_\varphi = -\frac{\mu_0 q_0 \Gamma}{4r_m} \exp[-k(z-h)] \begin{cases} Y_1(kr_m) J_1(kr), & r \leq r_m \\ J_1(kr_m) Y_1(kr), & r > r_m \end{cases}, \quad (6)$$

in terms of the Bessel functions of the first and the second kind. In order to single out the solution (6), we treat our stationary problem as the limit case of very weak electromagnetic emission from the dust devil, by taking at infinite radii only outward propagating cylindrical waves. In the limit of  $k \rightarrow 0$  solution (6) exactly corresponds to that in section 2. For fixed values of  $\xi \equiv kr_m$ , the vertical component of magnetic field within the vortex core,

$$B_z = -\frac{\mu_0 q_0 \Gamma}{2\pi r_m^2} \left( \frac{\pi}{2} \xi Y_1(\xi) \right) J_0(kr) \exp[-k(z-h)], \quad (7)$$

attains its maximum in the vortex center just above the top of saltation level.

[20] In a nonstationary case, when  $q_-(z, t) = q_0(t) \exp[-k(z-h)]$ , the electric charge conservation law reads  $\partial_t q_- + (\sigma/\varepsilon_0) q_- + \partial_z(\bar{w} q_-) = 0$ . In the virtue of  $\bar{w}(z) = W = \text{const}$ , one has  $\partial_t q_- + (\sigma/\varepsilon_0) q_- + W \partial_z q_- = 0$ , which finally gives (compare to (5))

$$\dot{q}_0 = q_0 (kW - \sigma/\varepsilon_0). \quad (8)$$

[21] Consider a ‘‘typical’’ Martian dust devil with  $V_m \equiv v_m(h) = 30$  m s $^{-1}$ , taken at the top of a very thin saltation layer, and  $r_m = 50$  m [Balme and Greeley, 2006, Table 9] and apply  $W = V_m/2 = 15$  m s $^{-1}$ . The condition  $\dot{q}_0 = 0$  in (8) is satisfied for  $k^{-1} = W\varepsilon_0/\sigma \approx 53$  m; consequently,  $\xi \approx 0.94$  and  $Y_1(\xi) \approx -0.83$ . An account for the electric permittivity  $\varepsilon \approx 1.6\varepsilon_0$  of the Martian CO $_2$  atmosphere would not significantly influence these results; it could also be compensated by taking smaller  $W$ -values. We tentatively take the

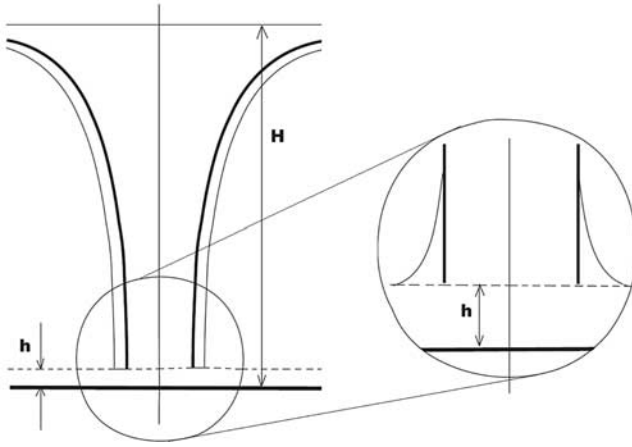


**Figure 3.** Schematic of negative electric charge distribution within the dust devil vortex model of section 2 (on the left). The distance between two closely adjacent curved lines, the thicker one representing the vortex core sidewalls, displays the constant electric charge density  $q_-$ . On the right, a slightly zoomed lower part of the modified vortex model of section 4 with an exponentially decaying  $q_-$  is analogously depicted. See more explanations in the text.

same electric charge vertical density  $|q_0| \sim 2 \times 10^{-4} \text{ C m}^{-1}$  as for terrestrial dust devils. To do it, we argue that the dust load (per unit volume) both on Earth and Mars approximately coincide [cf. *Fuerstenau*, 2006] and although the maximum electric charge on the particle in the Martian atmosphere is expected to be much smaller than on the Earth [*Farrell et al.*, 1999], this negative effect can be compensated (at least partially) by bigger size of Martian vortices, i.e., by greater number of particles at each horizontal level. In thus a way, we obtain  $(B_z)_{\max} \approx 3.0 \times 10^{-2} \text{ nT}$  (see section 2).

[22] It follows from (7) that the generated DC magnetic field is proportional to the vertical vorticity of the vortex,  $\omega_z = 2\Gamma/r_m^2$ . The latter quantity generally decreases along with the dust devil size increase, also when passing to gigantic, or extreme, Martian dust devils. It is explained by relatively weak dependency of the maximum wind velocity on the vortex size, approximately following the square root or even the cubic root law [*Balme and Greeley*, 2006]. So does the vertical velocity  $W$ , and gigantic dust vortices are associated with large  $\xi$ -values. An increasing factor  $\xi Y_1(\xi)$  in (7) is incapable of overweighting the impact of  $\omega_z$ -decrease; it only helps to maintain the magnetic field magnitude  $\sim 10^{-3} - 10^{-2} \text{ nT}$ . Additionally, because of the oscillating behavior of the Bessel functions at large  $\xi$ -values, even moderate variations in the electric dust devil parameters may lead to noticeable changes in the magnetic field in the vortex center. Possibly, it is a certain artifact of ascribing all the negatively charged particles to the vortex core edge vicinity, where they are moreover adjacent to the ground. The dust column can of course extend up to significant altitudes in the Martian atmosphere but our arguments give a hint that the electrically charged dust particles remain trapped in the vicinity of the ground at heights  $z \leq (2 - 3)k^{-1}$ .

[23] On the basis of their modeling results for the transient tribocharging spin-up process, *Zhai et al.* [2006]

deduced that the electric charge/electric field scales with the Martian dust devil size, the latter in contrast to our conclusions. In our opinion, it can partly be attributed to a specific choice of initial conditions of *Zhai et al.* [2006], where from the very beginning the triboelectrification region was virtually identified with the overall dust devil vortex domain. In our conceptual scheme we do not consider in detail the “spin-up”, or genesis, of electric dust devils but only assume that a steady-equilibrium electrostatic state has already been achieved. Also, in our work the triboelectrification region is effectively restricted to a relatively thin surface-adjacent saltation layer (see section 1 and Figure 1).

## 5. AC Magnetic Field Emission

[24] We saw in section 4 that high vorticity values are favorable for DC magnetic field generation. Inside the main dust devil vortex, such vorticity concentration occurs within smaller-scale secondary whirls [cf. *Bluestein*, 2005], also named the suction vortices after *Fujita* [1981]. These multiple vortices, or vortex filaments, which are also observed in direct numerical simulations of tornadoes [cf. *Lewellen et al.*, 2000], can serve as a possible source of AC magnetic emission [cf. *Houser et al.*, 2003]. To describe an individual vortex filament, take the limit  $r_m(z) \rightarrow 0$  in formulas of section 2, but keep constant the angular momentum  $\Gamma$  and the electric charge per unit height  $q_-$ , in order to get  $A = (1/4\pi)\mu_0 q_- \Gamma$ . The same result would follow if taking  $r_m^2(z) = r_m^2 = \text{const}$ , assuming the electric charge density  $\rho_e$  constancy within the vortex core and solving equation (2). Afterward, the limit of  $r_m \rightarrow 0$  should be performed for fixed  $\Gamma = v_m r_m$  and  $q_- = \rho_e \pi r_m^2$ .

[25] As an elementary mechanism to explain AC magnetic field generation, consider a pair of electrically charged vortex filaments, having the electric charge  $q_1 < 0$ ,  $q_2 < 0$  and the angular momentum  $\Gamma_1$ ,  $\Gamma_2$  of the same sign and being separated by the distance  $d$ . It is taken that  $\Gamma_1 > 0$  and  $\Gamma_2 > 0$ , without any loss. These two filaments permanently rotate about the common center of vorticity, at a point O, with the constant angular velocity  $\omega = (\Gamma_1 + \Gamma_2)/d^2$ . Electrostatic repulsive force between these charged filaments is of course neglected. It can readily be shown that in a point P, at the distance  $R \gg d$  from O, the dominating dipole component of AC magnetic field reads

$$B_z(R) \approx -\frac{\mu_0(q_1 - q_2)\Gamma_1\Gamma_2 d}{4\pi R^3(\Gamma_1 + \Gamma_2)} \cos\left(\frac{\Gamma_1 + \Gamma_2}{d^2}t - \vartheta_0\right), \quad (9)$$

where  $\vartheta_0$  is a constant phase angle. An AC magnetic field emission of the frequency  $f_M = (\Gamma_1 + \Gamma_2)/2\pi d^2$  is explained by different  $q$ -values, which may have filaments. For instance, for  $\Gamma_1 \approx \Gamma_2 \approx 10 \text{ m}^2 \text{ s}^{-1}$  and  $d \approx 1 \text{ m}$ , equation (9) shows that  $f_M \approx 3 \text{ Hz}$ . For  $|q_1 - q_2| \sim 2 \times 10^{-5} \text{ C m}^{-1}$  and at  $R \sim 10 d$ , the AC magnetic field amplitude is  $\sim 10^{-5} \text{ nT}$  and decays with distance as  $R^{-3}$ , whereas experimental data by *Houser et al.* [2003] and *Farrell et al.* [2004] show  $R^{-2.4}$ .

[26] However, the field observations by *Houser et al.* [2003] and *Farrell et al.* [2004] are seemingly more relevant to a horizontal magnetic field component (W. Farrell, personal communication, 2006). To interpret it, we truncate

the two filaments with magnetic fluxes  $\Phi_i = (1/2)\mu_0 q_i \Gamma_i$ ,  $i = 1, 2$ , at the top of a thin saltation layer, i.e., at a small height above the ground (see section 3). By making simple use of the Gauss divergence theorem, one obtains in the same point P the AC radial dipole magnetic field, given by the formula identical to (9).

[27] The two vortex filaments will also generate sound waves of the frequency  $f_A = (\Gamma_1 + \Gamma_2)/\pi d^2$  [cf. *Klyatskin*, 1966; *Gryanik*, 1983], which exemplifies Lighthill's aerodynamic mechanism of sound wave generation [e.g., *Crighthon*, 1981]. The intensity of acoustic emission per unit height is  $I = 16\pi^2 \rho \Gamma_1^2 \Gamma_2^2 (\Gamma_1 + \Gamma_2)^{-1} d^{-2} \text{Ma}^4$  [cf. *Klyatskin*, 1966; *Gryanik*, 1983], where  $\text{Ma} = (\Gamma_1 + \Gamma_2)/2c_0 d$  is the Mach number with the sound velocity  $c_0$  in its definition;  $\rho$  is the air density. In the considered case of the two linear vortex filaments, the acoustic emission is proportional to  $\text{Ma}^4$ , whereas in a general three-dimensional case it is proportional to  $\text{Ma}^5$ . In the wave far zone, at  $R \geq \pi c_0/\omega$ , one gets an estimate  $\overline{p'^2}/p^2 = 64\pi\kappa^{-2}(d/R)\Gamma_1^2\Gamma_2^2(\Gamma_1 + \Gamma_2)^{-4} \text{Ma}^7$  by equating  $I$  to the outward acoustic energy flux across a cylinder of radius  $R$  and unit height,  $(\overline{p'^2}/\rho c_0^2)c_0 2\pi R$ . Here,  $p'$  is the pulsation of pressure in the wave and an over-bar denotes averaging over the wave time period;  $p$  is the surface air pressure and  $\kappa$  the ratio of specific heats. In the terrestrial atmosphere  $\kappa = 1.4$ ,  $c_0 \approx 340 \text{ m s}^{-1}$  and for the above values  $\Gamma_1 \approx \Gamma_2 \approx 10 \text{ m}^2 \text{ s}^{-1}$ ,  $d \approx 1 \text{ m}$  one gets  $\text{Ma} \approx 1/34$ . If  $R = 100 \text{ m}$  is used then an estimate emerges,  $\sqrt{\overline{p'^2}/p^2} \approx 2.0 \times 10^{-6}$ , which corresponds to a rather loud sound of 80 db. In synthesis, we conjecture that if the considered scenario of AC magnetic emission plays a role, then an acoustic emission from the dust devil with a doubled frequency  $f_A = 2f_M$  ought to simultaneously be detected.

[28] In a real dust devil vortex, with its multiple secondary whirls of total number  $N$ , one would have a complex transient process of dynamical interaction between  $N$ -vortices [cf. *Newton*, 2001], naturally explaining the observed broadband magnetic emission of *Houser et al.* [2003]. Only in special circumstances, this interaction could be reduced to the above-analyzed simple interaction between a pair of vortices, giving rise to monochromatic magnetic emission, which is more consistent to field observations by *Farrell et al.* [2004].

[29] It is of some interest to assess theoretically the possible role of the Earth magnetic field on the ULF emission arising in association with dust devils (e.g., observed by *Houser et al.* [2003] in Nevada desert). First, we estimate the Lorentz force which acts on rotating electrically charged vortex filaments in the terrestrial magnetic field having the vertical component  $B_z^T$  of magnitude  $\sim 10^{-5} \text{ T}$ . For  $\Gamma_1 = \Gamma_2 = \Gamma$  the magnitude of Lorentz force acting on a filament with the electric charge density  $q_i$ ,  $i = 1, 2$ , and vertical extension  $H$  is given by a formula  $L_i = |q_i| H T d^{-1} |B_z^T|$ . For the above-used physical parameter values it yields  $L_i \sim 10^{-6} \text{ N}$ . Second, in an electric dust devil of section 2 the total radial Ampère force that tends to either expand or contract the vortex and which direction depends on (1) the sense of vortex rotation and (2) the sign of  $B_z^T$ , is given by the formula  $F_r = (4\pi/3) q_- \Gamma H r_m^{-1} B_z^T$ . For parameter values of section 2 and  $B_z^T = -10^{-5} \text{ T}$  (for the Northern Hemisphere) one gets the centrifugal/centripetal Ampère force of magnitude  $F_r \sim 8 \times 10^{-6} \text{ N}$  for cyclonic/anticy-

clonic vortices, respectively. Third, for a nonstationary model (5) with nonzero vertical electric currents  $J$ , the horizontal component  $B_h^T$  of terrestrial magnetic field, having generally the same magnitude as  $B_z^T$ , starts playing the role. For maximal possible misbalance between  $W$  and  $H\sigma/\epsilon_0$ , namely when the Ohmic dissipation is switched off, the appearing horizontal (lateral) component of the Ampère force does not exceed  $JHB_h^T \sim |q_-| HWB_h^T \sim 10^{-6} \text{ N}$ ; the latter being comparable with  $L_i$  and  $F_r$ . In all three cases the electromagnetic forces are by orders of magnitude less than the fluid dynamical forces including frictional forces, given the fact that under typical conditions the Earth's surface square meter is affected from aside the atmosphere by a horizontal force of 0.1 N. Therefore it is most likely that the role of the Earth magnetic field on the ULF emission arising in association with dust devils is quite minor, but it may be substantial in magnetic measurements because only time-variable part of magnetic emission from dust devils can actually be recorded in the presence of a rather strong ambient terrestrial magnetic field. It can be either ULF emission due to nonstationary processes discussed in this section, or slow time variations of DC-type magnetic field when the electric dust devil travels with steering wind flow relative to a ground-based magnetometer. A very small local magnetic field on Mars, order of nano-Tesla, will not be playing any role on the ULF magnetic emission from Martian dust devils. On the other hand, the Martian magnetic field smallness might favor increasing of possible impact of these magnetic emissions on Martian environments and also facilitate their direct measurements, especially from nearly immobile steady state vortices.

## 6. Conclusions

[30] Our study showed the following:

[31] 1. Simple analytical model of the dust devil vortex as a magnetic solenoid can be constructed to explain the DC magnetic field generation of measurable magnitude. This model is augmented with a simple 1-D model capable of describing the electric charge steady vertical distribution.

[32] 2. For relatively low electric conductivity of air on Earth, the model permits steady uniform vertical distribution of negative electric charge within the terrestrial dust devil vortex, up to its limit height, by also taking into account the vortex core expansion with altitude.

[33] 3. For high electric conductivity of air on Mars, the model modified onto an account of nonuniform electric charge vertical distribution hints on a rapid decay with altitude of dust grains electrification within Martian dust devils, with e-folding height of order of several tens of meters, which is significantly less than the total dust column height, especially in gigantic vortices.

[34] 4. Certain characteristic features of experimentally discovered ULF magnetic emission from the terrestrial dust devil [*Houser et al.*, 2003; *Farrell et al.*, 2004] can be interpreted in terms of dynamical interaction between multiple small-scale negatively charged vortex filaments ("suction vortices") inside the main dust devil vortex. This ULF magnetic emission should be accompanied by Lighthill's acoustic emission of approximately doubled frequency. It could serve as an observational test for the proposed mechanism validity.

[35] 5. The possible role of the Earth magnetic field on the ULF magnetic emission arising in association with dust devils is quite minor, but it may be substantial in magnetic measurements because only a time-dependent magnetic signal from dust devils can actually be recorded in the presence of a terrestrial magnetic field. It can be either AC magnetic emission due to nonstationary processes within dust devils (see section 5) or time variations of DC-type magnetic field (see section 2) when a dust devil travels with wind relative to a ground-based magnetometer.

[36] **Acknowledgments.** The work was supported by FONDECYT (Chile) under grant 1061002. We are grateful to two anonymous reviewers for their helpful comments and suggestions.

## References

- Balme, M., and R. Greeley (2006), Dust devils on Earth and Mars, *Rev. Geophys.*, *44*, RG3003, doi:10.1029/2005RG000188.
- Bluestein, H. B. (2005), A review of ground-based, mobile, W-band Doppler-radar observations of tornadoes and dust devils, *Dyn. Atmos. Oceans*, *40*(3), 163–188.
- Brooks, E. M. (1951), Tornadoes and related phenomena, in *Compendium of Meteorology*, edited by T. F. Malone, pp. 673–680, Am. Meteorol. Soc., Washington, D. C.
- Crighton, D. G. (1981), Acoustics as a branch of fluid mechanics, *J. Fluid Mech.*, *106*, 261–298.
- Farrell, W. M., and M. D. Desch (2001), Is there a Martian atmospheric electric circuit?, *J. Geophys. Res.*, *106*(E4), 7591–7596.
- Farrell, W. M., M. L. Kaiser, M. D. Desch, J. G. Houser, S. A. Cummer, D. M. Wilt, and G. A. Landis (1999), Detecting electrical activity from Martian dust storms, *J. Geophys. Res.*, *104*(2), 3795–3801.
- Farrell, W. M., G. T. Delory, S. A. Cummer, and J. R. Marshall (2003), A simple electrodynamic model of a dust devil, *Geophys. Res. Lett.*, *30*(20), 2050, doi:10.1029/2003GL017606.
- Farrell, W. M., et al. (2004), Electric and magnetic signatures of dust devils from the 2000–2001 MATADOR desert tests, *J. Geophys. Res.*, *109*, E03004, doi:10.1029/2003JE002088.
- Farrell, W. M., J. R. Marshall, S. A. Cummer, G. T. Delory, and M. D. Desch (2006), A model of the ULF magnetic and electric field generated from a dust devil, *J. Geophys. Res.*, *111*, E11004, doi:10.1029/2006JE002689.
- Fuerstenau, S. D. (2006), Solar heating of suspended particles and the dynamics of Martian dust devils, *Geophys. Res. Lett.*, *33*, L19S03, doi:10.1029/2006GL026798.
- Fujita, T. T. (1981), Tornadoes and downbursts in the context of generalized planetary scales, *J. Atmos. Sci.*, *38*(8), 1511–1534.
- Gryanik, V. M. (1983), Emission of sound by linear vortical filaments, *Izv. Atmos. Ocean. Phys.*, *19*(2), 150–152.
- Houser, J. G., W. M. Farrell, and S. M. Metzger (2003), ULF and ELF magnetic activity from a terrestrial dust devil, *Geophys. Res. Lett.*, *30*(1), 1027, doi:10.1029/2001GL014144.
- Klyatskin, V. I. (1966), Sound emission by a system of vortices (in Russian), *Izv. Akad. Nauk SSSR, Mekh. Zhidk. Gasa*, *6*, 87–92.
- Kurgansky, M. V. (2005), A simple model of dry convective helical vortices (with applications to the atmospheric dust devil), *Dyn. Atmos. Oceans*, *40*(3), 151–162.
- Lewellen, D. C., W. S. Lewellen, and J. Xia (2000), The influence of a local swirl ratio on tornado intensification near the surface, *J. Atmos. Sci.*, *57*, 527–544.
- Newton, P. K. (2001), *The N-Vortex Problem: Analytical Techniques*, 420 pp., Springer, New York.
- Rennó, N. O., M. L. Burkett, and M. P. Larkin (1998), A simple thermodynamical theory for dust devils, *J. Atmos. Sci.*, *55*, 3244–3252.
- Sinclair, P. C. (1966), A quantitative analysis of the dust devil, Ph.D. dissertation, 292 pp., Univ. of Ariz., Tucson.
- Sinclair, P. C. (1973), The lower structure of dust devils, *J. Atmos. Sci.*, *30*, 1599–1619.
- Toigo, A. D., M. I. Richardson, S. P. Ewald, and P. J. Gierasch (2003), Numerical simulation of Martian dust devils, *J. Geophys. Res.*, *108*(E6), 5047, doi:10.1029/2002JE002002.
- Zhai, Y., S. A. Cummer, and W. M. Farrell (2006), Quasi-electrostatic field analysis and simulation of Martian and terrestrial dust devils, *J. Geophys. Res.*, *111*, E06016, doi:10.1029/2005JE002618.

L. Baez, M. V. Kurgansky, and E. M. Ovalle, Department of Geophysics, Faculty of Physical and Mathematical Sciences, University of Concepción, Casilla-160C, Concepción, Chile. (lbaez@udec.cl; kurgansk@udec.cl; eo@dgeo.udec.cl)